Preprints of the 19th World Congress
The International Federation of Automatic Control
Cape Town, South Africa. August 24-29, 2014

Two-sided wave-absorbing control of a heterogenous vehicular platoon ⋆

Dan Martinec * **Ivo Herman** * **Michael Šebek** *

* *All authors are with Department of Control Engineering, Czech Technical University in Prague, Czech Republic.*

Abstract: The paper tailors the so-called wave-absorbing control designed for a homogenous platoon of vehicles to a platoon where dynamics of vehicles differ. The proposed solution is based on the symmetric bidirectional control of the in-platoon vehicles and wave-absorbing control of the platoon ends. This type of control reduces oscillations of vehicle's velocities and significantly decrease the settling time of the platoon by absorbing waves on the platoon ends. The necessary transfer-function-based mathematical apparatus for description of the so-called soft boundary is also presented. Although the soft boundary is a virtual boundary located between the vehicles of different dynamics, it significantly alters the behaviour of the platoon. It is shown how to incorporate model of the soft boundary into the design of the wave-absorbing control such that its effect is minimized. The proposed control scheme is verified on numerous mathematical simulations.

Keywords: Wave-absorbing controller, heterogenous vehicular platoon, symmetric bidirectional control, soft boundary, wave transfer function.

1. INTRODUCTION

1.1 Vehicular platooning

The main task of the vehicular platooning is to drive safely and efficiently several vehicles travelling in a row. The motivation is to increase highways capacity, improve traffic safety and allow drivers to pay attention to other duties.

Regarding control strategies, a few papers considered centralized control approaches but much more attention has been given to fully or partially distributed control approaches; each vehicle then carries its own local onboard controller with only limited knowledge of state of the rest of the platoon. The *string stability* analysis serves as one of the basic performance analysis tool for a distributed approach. Although there are several definitions of string stability, for instance by Swaroop and Hedrick (1996), Eyre et al. (1998) or by Seiler et al. (2004), the underlying question is the same: Is the disturbance present at one vehicle amplified as it propagates in the platoon to other vehicles? For a string stable platoon, the answer is 'no', however, it is important to note that this does not guarantee that vehicles do not crash into each other. The definition of the string stability for heterogenous platoon was introduced in Shaw and Hedrick (2007) under the term *heterogenous string stability.*

This paper mostly relies on the so-called *symmetric bidirectional control*, where each vehicle equally weights information about distance to its immediate predecessor and successor. Although a homogenous platoon with a symmetric bidirectional control is string unstable as well, scaling of the disturbance amplification is qualitatively better than for the predecessor following algorithm. However, this comes at a price of a very long settling time as showed Middleton and Braslavsky (2010). Moreover, stability of such a platoon becomes an issue for a large number of vehicles due to the least stable closed-loop eigenvalue converging to zero as showed Barooah et al. (2009).

As for the heterogenous platoon, Middleton and Braslavsky (2010) showed that within reasonable confines the heterogeneity of the platoon has little effect on the string stability. However, the scalability is poor for a long platoon as showed by Herman et al. (2014). Another study of the heterogenous platoon was done by Lestas and Vinnicombe (2007), where the symmetric bidirectional control was enhanced by a weak coupling with the leader. The effect of both heterogeneity and asymmetry on the closed loop stability margin is examined in Hao and Barooah (2010).

1.2 Wave-absorbing controller

It is well known from the field of mechanics that a travelling wave appears in the response of flexible mechanical systems on various inputs. The wave travels in the system back and forth reflecting on the system boundaries. It is those reflections that usually degrades the system's performance and makes the behaviour undesirably oscillatory.

Among the first papers proposing a controller that would cancel the wave reflection on the structural ends was the work of Vaughan (1968). Later, the approach was reformulated in the term of traveling wave modes by Flotow (1986). Recently, a series of paper by O'Connor, see for instance O'Connor (2006), introduced yet another approach, the *wave-based control.* They described the travelling wave by the so-called *wave transfer function* and

⋆ The research was supported by the Grant Agency of the Czech Republic within the project GACR P103-12-1794.

adopted the travelling-wave principle for lumped multi-link flexible mechanical systems. Simultaneously, Halevi (2005) showed a similar approach for control of continuous flexible structures under the name *absolute vibration suppression*. The two aforementioned concepts are compared in the joint paper by Peled et al. (2012). Recently, paper by Martinec et al. (2013) introduces the so-called *wave-absorbing controller*, which tailors the wave-based control to the domain of vehicular platooning, where distances between vehicles have to be additionally considered, since there is no physical connection between the vehicles. The link between vehicles is made by a distance controller implemented onboard each vehicle.

1.3 Problem formulation

This paper extends the work of Martinec et al. (2013) by assuming more realistic conditions in terms of a heterogenous vehicular platoon, that means a platoon with vehicles that are not identical. The heterogeneity causes that the travelling wave partially reflects when it travels between the vehicles of different dynamics. The wave-absorbing controller can be applied on platoon ends, however, effect of the boundary has to be considered when treating the reference signal for the controller. For simplicity, we assume a two types of vehicles; trucks and cars, though the result can be generalized even for a platoon where each vehicle has a different dynamics. It is convenient, as shown in the SARTRE project described by Coelingh and Solyom (2012), to order the platoon such that all trucks are located in the front and cars are located behind them, see Fig. 1. Such a platoon configuration is treated in this paper.

The paper has two contributions: a) It presents a mathematical ('transfer function') description of the so-called soft boundary and b) it shows how to efficiently control a heterogenous platoon by a wave absorber, specifically, it presents a way how to design the reference signals $X_{\mathrm{ref}}(s)$ and $X_{\mathrm{ref,rear}}(s)$.

2. MATHEMATICAL MODEL OF VEHICLES

Each vehicle is modelled as a double integrator with a simple (linear) model of friction, ξ. In the Laplace domain, the model reads as,

$$s^2 X_n(s) = -s\xi X_n(s) + U_n(s), \qquad (1)$$

where s is the Laplace variable, $X_n(s)$ represents a position of the nth vehicle and $U_n(s)$ is the system input which is generated by the platoon controller specified in the following.

We assume that each in-platoon vehicle is controlled by a symmetric bidirectional controller, that means it is capable to measure distance to both its immediate predecessor and successor with task to equalize these distances. To regulate the distances without a steady state error, the vehicles need to be equipped with a PI or PID controller. It is sufficient to implement a PI controller because of the simple vehicle model, hence,

$$U_n(s) = \left(k_{\mathrm{p}} + \frac{k_{\mathrm{i}}}{s}\right)\left(D_{n-1}(s) - D_n(s)\right), \qquad (2)$$

where $D_n(s)$ is the distance between vehicles indexed n and $(n+1)$, $D_n(s) = X_n(s) - X_{n+1}(s)$, k_p and k_i are proportional and integral gains of the PI controller, respectively.

We substitute (2) into (1) and obtain the resulting model of the in-platoon vehicle,

$$X_n(s) = \frac{k_{\mathrm{p}}s + k_{\mathrm{i}}}{s^3 + \xi s^2 + 2k_{\mathrm{p}}s + 2k_{\mathrm{i}}}(X_{n-1} + X_{n+1}). \qquad (3)$$

The vehicle at the rear end, indexed as N, is controlled either by the wave-absorbing controller, see the next section, or by the so-called predecessor following algorithm,

$$X_N(s) = \frac{k_p s + k_i}{s^3 + \xi s^2 + k_p s + k_i}(X_{N-1}(s) - D_{\mathrm{ref}}(s)), \qquad (4)$$

where $D_{\mathrm{ref}}(s)$ is the reference/desired distance between vehicles. Its task is to keep the distance to the immediate predecessor equal to the reference distance.

We assume that there are two types of vehicles in the platoon, trucks and cars. The coefficients of the systems are summarized in Table. 1. The coefficients of the PI algorithms were tuned such that the local system of the vehicle is stable without long transient.

Table 1. Truck's and car's coefficients of the vehicle models (3) and (4).

Vehicle type	Coefficient of the vehicular model
Truck	$\xi_{\mathrm{t}} = 2\,\mathrm{Nsm}^{-1}$, $k_{\mathrm{p,t}} = 1\,\mathrm{Nm}^{-1}$, $k_{\mathrm{i,t}} = 1\,\mathrm{Ns}^{-1}\mathrm{m}^{-1}$
Car	$\xi_{\mathrm{c}} = 4\,\mathrm{Nsm}^{-1}$, $k_{\mathrm{p,c}} = 4\,\mathrm{Nm}^{-1}$, $k_{\mathrm{i,c}} = 4\mathrm{Ns}^{-1}\mathrm{m}^{-1}$

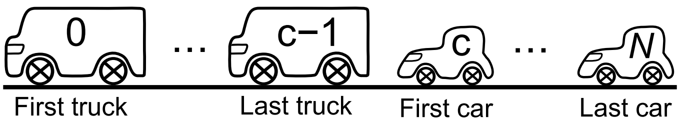

Fig. 1. Heterogenous platoon of $(N+1)$ vehicles with c trucks in the front and $(N-c)$ cars behind them. The leader of the platoon, a truck, is indexed 0, while the index of the first car in the platoon is c.

3. WAVE ABSORBING CONTROLLER

This paper continues in the work of Martinec et al. (2013). For convenience of the reader, we will briefly review the main results of the paper.

In a platoon of identical vehicles, the position of the nth vehicle composed of two parts, $A_n(s)$ and $B_n(s)$, that represent two waves propagating along a platoon in the forward and backward directions, respectively. We assume a platoon of infinitely many vehicles, hence there is no reflection on platoon ends. The mathematical model of such a platoon is

$$X_n(s) = A_n(s) + B_n(s), \qquad (5)$$
$$A_{n+1}(s) = G(s)A_n(s), \qquad (6)$$
$$B_n(s) = G^{-1}(s)B_{n-1}(s), \qquad (7)$$

where $G(s)$ is the so-called wave transfer function. In other words, the wave transfer function describes how the wave propagates from vehicle to vehicle in the platoon. The wave transfer function expressed for the model (3) is

$$G(s) = \frac{s^3 + \xi s^2 + 2k_p s + 2k_i}{2(k_p s + k_i)} - \frac{s\sqrt{s^4 + 2\xi s^3 + \xi^2 s^2 + 4k_p s^2 + 4k_p \xi s + 4k_i s + 4k_i \xi}}{2(k_p s + k_i)}. \tag{8}$$

We label $G(s)$ to be the wave transfer function for a platoon of trucks and $H(s)$ to be the wave transfer function for a platoon of cars.

Any type of a wave-absorbing controller can be designed, however, the reference signal for the controller is different for each case. In this paper, we employ the *Two-sided wave-absorbing controller*, i.e. both platoon ends absorb the incoming wave, therefore, the wave can reflect only on the soft boundary. This clearly demonstrates effect of the soft boundary. The Two-sided wave-absorbing controller is described as

$$X_\mathrm{f}(s) = X_\mathrm{ref}(s) + G(s)B_1(s) = X_\mathrm{ref}(s)\left(1 - G^2(s)\right) + G(s)X_1(s), \tag{9}$$

$$X_\mathrm{r}(s) = X_\mathrm{ref,rear}(s) + H(s)A_{N-1}(s) = X_\mathrm{ref,rear}(s)\left(1 - H^2(s)\right) + H(s)X_{N-1}(s), \tag{10}$$

where $X_\mathrm{f}(s)$ is input to the positional controller of the leader, $X_\mathrm{ref}(s)$ is a reference signal with ramp of slope w_f. Input to the rear-end vehicle is denoted by $X_\mathrm{r}(s)$ with reference signal $X_\mathrm{ref,rear}(s)$ with slope w_r.

In order to implement the wave-absorbing controller, we need to find an impulse response of the wave transfer function. Due to the square root function of a polynomial, it is a very challenging task. However, we can find an approximation in the time domain in form of a finite impulse response (FIR) filter. The main idea is to approximate the wave transfer function with a rational transfer function $G^l(s)$ derived by the following recursive formula

$$G^l(s) = \frac{k_\mathrm{p}s + k_\mathrm{i}}{s^3 + \xi s^2 + 2k_\mathrm{p}s + 2k_\mathrm{i} - (k_\mathrm{p}s + k_\mathrm{i})G^{l-1}(s)}. \tag{11}$$

Then carry out the impulse response of $G^l(s)$, truncate it and sample it with a sufficient frequency to obtain a FIR filter coefficients.

4. SOFT BOUNDARY

Apart from the forced/free end boundary on the platoon ends, there is yet another boundary located between the last truck and the first car, which originates from the different dynamics of the vehicles. We call such a boundary a *soft boundary*. Although a soft boundary is virtual in nature, it fundamentally affects the platoon behaviour.

Even though we assume that each vehicle is modelled as a double integrator with a linear friction, the presented mathematical model of the soft boundary is valid for arbitrary vehicle dynamics, since the mathematical derivation is carried out with general $G(s)$ and $H(s)$.

4.1 Mathematical model of the soft boundary

When a wave is travelling through a boundary between two media of different densities, part of the wave is reflected back from the boundary while part gets through, this phenomenon is known from basic wave physics, see for instance French (2003). The same situation occurs on the soft boundary between the last truck and the first car. To mathematically describe what happens when a wave reaches the soft boundary, we need in total four transfer functions. The transfer functions are summarized in Table 2 and depicted in Fig. 2.

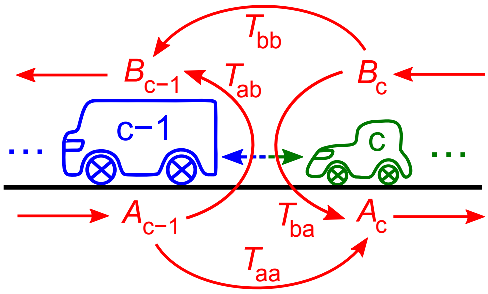

Fig. 2. Scheme of reflections on a soft boundary inside a platoon described by (12a) and (12b).

Table 2. List of the transfer functions describing reflection on a soft boundary. For the DC gain, we assume a ramp signal on the input.

Label	Description	Trans. fun.	DC gain
T_aa	$A_\mathrm{c-1} \to A_\mathrm{c}$	$\frac{H - HG^2}{1 - HG}$	κ_aa
T_ab	$A_\mathrm{c-1} \to B_\mathrm{c-1}$	$\frac{HG - G^2}{1 - HG}$	κ_ab
T_ba	$B_\mathrm{c} \to A_\mathrm{c}$	$\frac{HG - H^2}{1 - HG}$	κ_ba
T_bb	$B_\mathrm{c} \to B_\mathrm{c-1}$	$\frac{G - H^2G}{1 - HG}$	κ_bb

The mathematical derivation for the soft boundary is given in the appendix. The resulting model is

$$A_\mathrm{c} = A_\mathrm{c-1}\frac{H - HG^2}{1 - HG} + B_\mathrm{c}\frac{HG - H^2}{1 - HG}, \tag{12a}$$

$$B_\mathrm{c-1} = B_\mathrm{c}\frac{G - H^2G}{1 - HG} + A_\mathrm{c-1}\frac{HG - G^2}{1 - HG}. \tag{12b}$$

Transfer functions describing reflection on the soft boundary are related,

$$T_\mathrm{aa} + T_\mathrm{bb} = G + H, \tag{13}$$

$$(T_\mathrm{aa} + T_\mathrm{bb})(G - T_\mathrm{aa}) = T_\mathrm{ba} - T_\mathrm{ab}, \tag{14}$$

$$(T_\mathrm{aa} + T_\mathrm{bb})(H - T_\mathrm{bb}) = T_\mathrm{ab} - T_\mathrm{ba}, \tag{15}$$

which yield the following relations between their DC gains

$$\kappa_\mathrm{aa} = 2 - \kappa_\mathrm{bb}, \quad \kappa_\mathrm{ab} = 1 - \kappa_\mathrm{bb}, \quad \kappa_\mathrm{ba} = 1 - \kappa_\mathrm{aa}. \tag{16}$$

Values of DC gains expressed for the model (3) are given in the appendix.

4.2 Numerical simulations of the soft boundary

This subsection verifies the model of the soft boundary (12a), (12b) through the mathematical simulation in the following manner. First, we simulate reaction of the platoon on given input signal, in our case it is acceleration of the leader or the rear-end vehicle. Second, we carry out the reaction of the platoon on the same input signal with the 'wave' mathematical model (5)–(7), (12a) and (12b). At last, we compare results of these two methods.

We simulate a platoon with 5 trucks and 4 cars, that means the soft boundary is located between vehicles indexed 4 and 5. To fully demonstrate effect of the soft boundary, we equip both platoon ends with the wave-absorbing controller. For this case, we disregard the reference velocity and distance signals. We only command the leader or the rear-end vehicle to accelerate to a velocity of $1\,\mathrm{ms}^{-1}$.

Fig. 3 shows velocities of the last truck and the first car for the whole time of the simulations. We can see that as the wave travels from the left, it gets amplified by factor of $\kappa_{\mathrm{aa}} \approx 1.171$ while when it travels from the opposite direction it is attenuated by factor of $\kappa_{\mathrm{bb}} \approx 0.828$, i.e. the amplitude is attenuated. We can see an agreement between the soft-boundary-derived and independently-simulated velocities. Fig. 4 compares behaviour of the platoon with and without the soft boundary.

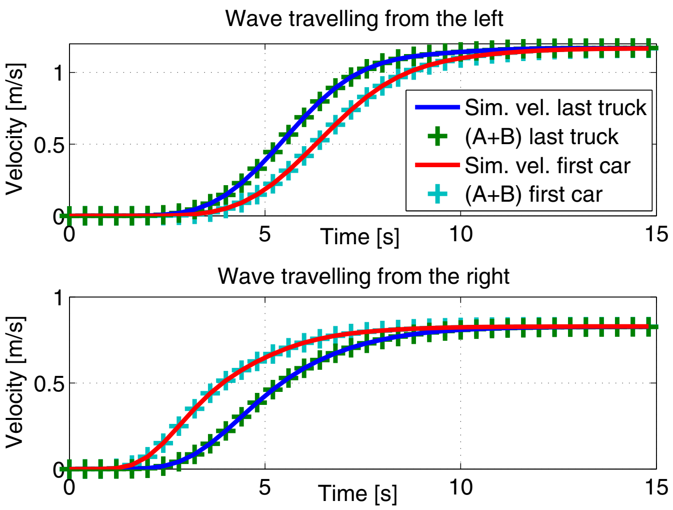

Fig. 3. Velocity of the last truck and the first car simulated by the Matlab Simulink (solid lines) compared to the velocity components computed before the simulation using (12a) and (12b) (crosses). The top panel shows situation when the leader accelerates to a velocity of $1\,\mathrm{ms}^{-1}$ which initiates a wave propagating to the soft boundary from the left, i.e. from trucks to cars. The opposite situation is shown in the bottom panel where the rear-end vehicle initiates a wave by accelerating at $1\,\mathrm{ms}^{-1}$.

5. TWO-SIDED WAVE-ABSORBING CONTROLLER

5.1 *Design of the controller*

The principle how to absorb the incoming wave on the platoon end is the same as for a homogenous platoon. Similarly, slopes of the reference signals determine the steady state velocity of the whole platoon, $v(\infty)$, and the inter-vehicle distances, $d(\infty)$. However, the steady states are changed by the soft boundary as we can see in Fig. 3. We can compensate its effect by incorporating DC gains from Table 2 into slopes of the reference signals.

We assume that the platoon ends are controlled by the wave-absorbing controllers (9), (10), then combining (12a), (12b) and (A.7) yields the platoon steady states

$$\begin{aligned} v(\infty) &= (1+\kappa_{\mathrm{ab}})w_{\mathrm{f}} + \kappa_{\mathrm{bb}}w_{\mathrm{r}}, \\ &= \kappa_{\mathrm{aa}}w_{\mathrm{f}} + (1+\kappa_{\mathrm{ba}})w_{\mathrm{r}}, \qquad (17)\\ d(\infty) &= \kappa_{\mathrm{d}}w_{\mathrm{f}} - \kappa_{\mathrm{d}}w_{\mathrm{r}}. \qquad (18) \end{aligned}$$

We can interpret it in the following way. The steady state velocity of the whole platoon is composed of the three parts: i) initial commanded velocity to the leader w_{f}, ii) part of velocity w_{f} that reflects from the soft boundary back to the leader, iii) initial commanded velocity to the rear-end vehicle, w_{r}, that is amplified on the soft boundary. The steady state distance between vehicles is composed of two parts which follows from (A.8).

We substitute $v_{\mathrm{ref}}/d_{\mathrm{ref}}$ for $v(\infty)/d(\infty)$ and express $w_{\mathrm{f}}/w_{\mathrm{r}}$ from (17)/(18). This gives slopes for the reference inputs of the Two-sided wave-based controller as,

$$w_{\mathrm{f}} = \frac{1}{2}v_{\mathrm{ref}} + \frac{1}{2}\frac{\kappa_{\mathrm{bb}}}{\kappa_{\mathrm{d}}}d_{\mathrm{ref}}, \quad w_{\mathrm{r}} = \frac{1}{2}v_{\mathrm{ref}} - \frac{1}{2}\frac{\kappa_{\mathrm{aa}}}{\kappa_{\mathrm{d}}}d_{\mathrm{ref}}. \qquad (19)$$

5.2 *Numerical simulations*

Similarly as in Section 4.2, we assume a platoon of 9 vehicles, where first 5 vehicles are trucks and following 4 vehicles are cars. This means that the soft boundary is located between vehicles indexed 4 and 5.

First, we will show performance of the platoon without any absorber, i.e. the leader travels with constant velocity and the rear-end vehicle is described by (4). Simulation of acceleration of this a platoon is shown in Fig. 5. We can see that the settling time is very long since it scales quadratically with the number of vehicles as shown by Martinec et al. (2013).

Simulation of the platoon with the Two-sided wave-absorbing controller is shown in Fig. 6. The settling time is significantly decreased, since now it scales linearly with the number of vehicles.

6. CONCLUSION

The paper presents a transfer-function-based mathematical description of the so-called soft boundary located in a platoon between two vehicles of different dynamics, where each in-platoon vehicle is controlled by the symmetric bidirectional controller. Although the boundary is virtual, it has a profound effect on the platoon behaviour. As in case of the homogenous platoon, it is beneficial to use a wave-absorbing platoon control. However, effect of the soft boundary needs to be considered for carrying out slopes of the reference signals.

The proposed approach is demonstrated on a platoon with two types of vehicles but it can be generalized for a platoon where each vehicle has a different dynamics.

On the mathematical simulations are shown that advantages of a wave-absorbing control of a heterogenous platoon remains the same. That means reduction of the settling time by eliminating oscillations in velocity of the platoon vehicles. Another benefit is that the control is fully decentralized and require no wireless communication between vehicles. The paper discuss only the Two-sided wave-absorbing control but it can be modified for other types of the wave-absorbing control as well.

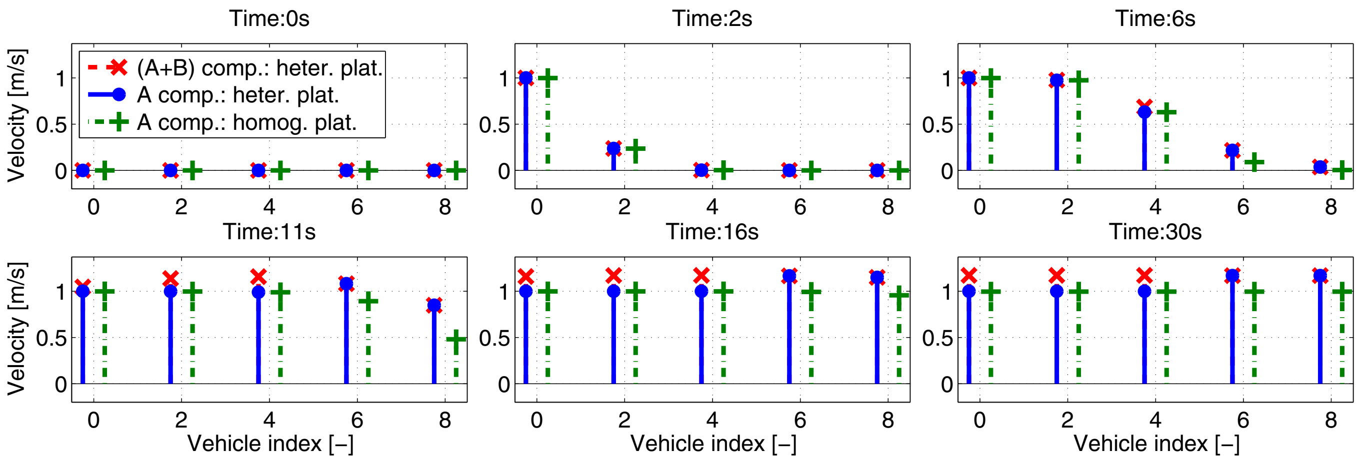

Fig. 4. Simulation of the velocity wave propagating in the platoon with the soft boundary located between vehicles indexed 4 and 5 and in the platoon without the soft boundary where all vehicles are trucks, i.e. a homogenous platoon. At the beginning, $t = 0\,\mathrm{s}$, all vehicles are standing still except for the leader which accelerates to a velocity $1\,\mathrm{ms}^{-1}$. At intermediate times, the wave travels to the soft boundary, where it is partially reflected and partially amplified by κ_{bb}. By propagating back to the leader, it forces trucks to accelerate by another κ_{ab}. The waves are absorbed on the platoon ends by the wave-absorbing controller, therefore, there is no B component in the homogenous platoon or for cars in the heterogenous platoon. The red crosses represent the derivation of $A + B$ positional components computed from the soft boundary model (12a) and (12b), the green plus signs are derivations of A components in the homogenous platoon of trucks computed from model (5)–(7). The B components of all the vehicles are equal to zero in the homogenous platoon because there is no boundary where the wave can reflect.

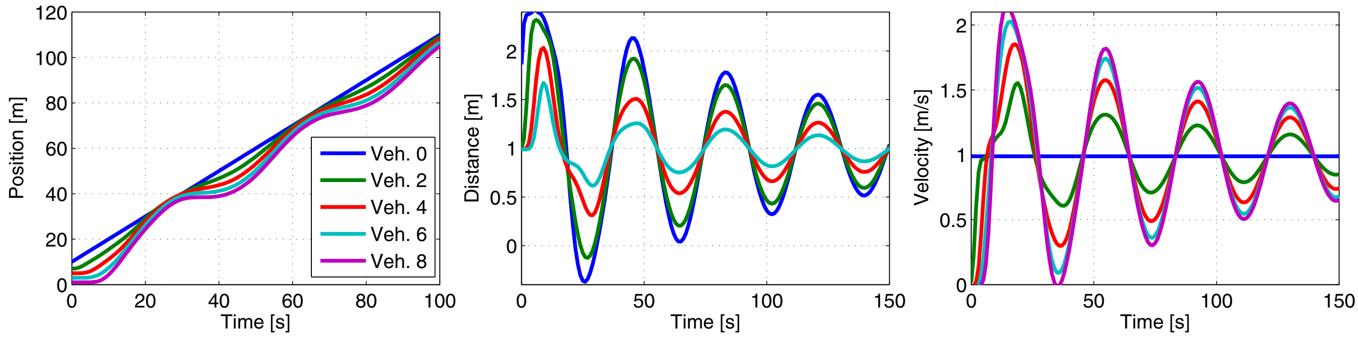

Fig. 5. Simulation of the platoon without the wave-absorbing controller when the leader accelerates to velocity $v_{\mathrm{ref}} = 1\,\mathrm{ms}^{-1}$. The reference distance is kept fixed, $d_{\mathrm{ref}} = 1\,\mathrm{m}$, for the whole time.

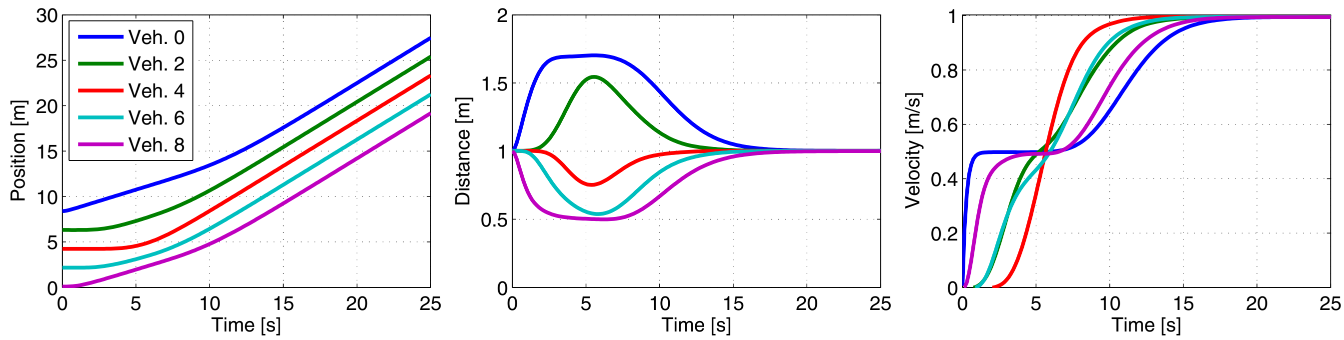

Fig. 6. Simulation of the platoon with the wave-absorbing controller implemented on both platoon ends. The platoon is commanded to accelerate to velocity $v_{\mathrm{ref}} = 1\,\mathrm{ms}^{-1}$ while the reference distance is kept fixed, $d_{\mathrm{ref}} = 1\,\mathrm{m}$.

The performance of the controller in the presence of modelling errors and disturbances is subject of further research.

REFERENCES

Barooah, P., Mehta, P., and Hespanha, J. (2009). Mistuning-Based Control Design to Improve Closed-Loop Stability Margin of Vehicular Platoons. *IEEE Transactions on Automatic Control*, 54(9), 2100–2113.

Coelingh, E. and Solyom, S. (2012). All aboard the robotic road train. *IEEE Spectrum*, 49(11), 34–39.

Eyre, J., Yanakiev, D., and Kanellakopoulos, I. (1998). A Simplified Framework for String Stability Analysis of Automated Vehicles. *Vehicle System Dynamics*.

Flotow, A.H. (1986). Traveling wave control for large spacecraft structures. *Journal of Guidance Control and Dynamics*, 9(4), 462–468.

French, A.P. (2003). *Vibration's and Waves*. M.I.T. introductory physics series. CBS Publishers & Distributors.

Halevi, Y. (2005). Control of Flexible Structures Governed by the Wave Equation Using Infinite Dimensional Transfer Functions. *Journal of Dynamic Systems, Measurement, and Control*, 127(4), 579.

Hao, H. and Barooah, P. (2010). Control of large 1D networks of double integrator agents: Role of heterogeneity and asymmetry on stability margin. In *49th IEEE Conference on Decision and Control (CDC)*, 7395–7400. IEEE.

Herman, I., Martinec, D., Hurák, Z., and Sebek, M. (2014). Harmonic instability of asymmetric bidirectional control of a vehicular platoon. *(Accepted to the) 2014 American Control Conference*.

Lestas, I. and Vinnicombe, G. (2007). Scalability in heterogeneous vehicle platoons. *2007 American Control Conference*, (M), 4678–4683.

Martinec, D., Herman, I., Hurák, Z., and Šebek, M. (2013). Wave-absorbing vehicular platoon controller. *eprint arXiv:1311.2095*.

Middleton, R.H. and Braslavsky, J.H. (2010). String Instability in Classes of Linear Time Invariant Formation Control With Limited Communication Range. *IEEE Transactions on Automatic Control*, 55(7), 1519–1530.

O'Connor, W.J. (2006). Wave-echo control of lumped flexible systems. *Journal of Sound and Vibration*, 298(4-5), 1001–1018.

Peled, I., O'Connor, W., and Halevi, Y. (2012). On the relationship between wave based control, absolute vibration suppression and input shaping. *Mechanical Systems and Signal Processing*, 1–11.

Seiler, P., Pant, A., and Hedrick, K. (2004). Disturbance Propagation in Vehicle Strings. *IEEE Transactions on Automatic Control*, 49(10), 1835–1841.

Shaw, E. and Hedrick, J.K. (2007). String Stability Analysis for Heterogeneous Vehicle Strings. *2007 American Control Conference*, 3118–3125.

Swaroop, D. and Hedrick, J. (1996). String stability of interconnected systems. *IEEE Transactions on Automatic Control*, 41(3), 349–357.

Vaughan, D.R. (1968). Application of Distributed Parameter Concepts to Dynamic Analysis and Control of Bending Vibrations. *Journal of Basic Engineering*, 90(2), 157–166.

Appendix A. MATHEMATICAL DERIVATION OF REFLECTION ON A SOFT BOUNDARY

This technical result follow the mathematical derivation of reflection on a forced boundary derived by Martinec et al. (2013). The model of a forced boundary was carried out to be $A_1 = GX_0 - G^2B_1$. We can apply this result and describe model of the last truck and the first car from Fig. 1 and Fig. 2 as

$$A_\mathrm{c} = -H^2B_\mathrm{c} + H_1X_{\mathrm{c}-1}, \tag{A.1}$$

$$B_{\mathrm{c}-1} = -G_1^2A_{\mathrm{c}-1} + GX_\mathrm{c}. \tag{A.2}$$

Substituting (5) for $X_{\mathrm{c}-1}$ and (A.2) for $B_{\mathrm{c}-1}$ yields

$$A_\mathrm{c} = -H^2B_\mathrm{c} + H(A_{\mathrm{c}-1} - G^2A_{\mathrm{c}-1} + G(A_\mathrm{c} + B_\mathrm{c})). \tag{A.3}$$

Separating A_c gives the final result

$$A_\mathrm{c} = A_{\mathrm{c}-1}\frac{H - HG^2}{1 - HG} + B_\mathrm{c}\frac{HG - H^2}{1 - HG}. \tag{A.4}$$

Similarly, substituting (5) for $X_{\mathrm{c}-1}$ and (A.1) for A_c gives

$$B_{\mathrm{c}-1} = -G^2A_{\mathrm{c}-1} + G(-H^2B_\mathrm{c} + H(A_{\mathrm{c}-1} + B_{\mathrm{c}-1}) + B_\mathrm{c}). \tag{A.5}$$

Finally, separating B_n yields

$$B_{\mathrm{c}-1} = B_\mathrm{c}\frac{G - GH^2}{1 - HG} + A_{\mathrm{c}-1}\frac{HG - G^2}{1 - HG} \tag{A.6}$$

The distance between the last truck and the first car, D_c, is described as

$$D_\mathrm{c} = (1 + T_\mathrm{ab} - T_\mathrm{aa})G_1^{\mathrm{c}\text{-}1}A_0 + (T_\mathrm{bb} - T_\mathrm{ba} - 1)H^{N-\mathrm{c}}B_N. \tag{A.7}$$

The DC gain from A_0 to D_c, assuming a ramp signal of A_0, is

$$\kappa_\mathrm{d} = \lim_{s\to 0}\frac{D_\mathrm{c}}{A_0} = \lim_{s\to 0}\frac{1}{s}\frac{1 - H - G^2 + HG^2}{1 - HG} = 2\frac{\sqrt{\xi_\mathrm{c}\xi_\mathrm{t}k_\mathrm{i,c}k_\mathrm{i,t}}}{k_\mathrm{i,c}k_\mathrm{i,t}}\left(\frac{\sqrt{\xi_\mathrm{t}k_\mathrm{i,t}}}{k_\mathrm{i,t}} + \frac{\sqrt{\xi_\mathrm{c}k_\mathrm{i,c}}}{k_\mathrm{i,c}}\right)^{-1}. \tag{A.8}$$

It can be shown that the DC gain from B_N to D_c is $(-\kappa_\mathrm{d})$, if we assume that B_N is a ramp signal.

Appendix B. DC GAINS OF THE SOFT BOUNDARY TRANSFER FUNCTIONS

We evaluate the DC gains from Table 2 for the vehicle dynamics described in (3).

The DC gain of T_aa is

$$\kappa_\mathrm{aa} = \lim_{s\to 0} T_\mathrm{aa} = \lim_{s\to 0}\frac{H - HG^2}{1 - HG} = \frac{0}{0}. \tag{B.1}$$

Applying L'Hopital's rule gives

$$\kappa_\mathrm{aa} = \lim_{s\to 0}\frac{H' - H'G^2 - 2HGG'}{-H'G - HG'}. \tag{B.2}$$

We substitute $\lim_{s\to 0}(G'(s)) = -\sqrt{\xi_\mathrm{t}k_\mathrm{i,t}}/k_\mathrm{i,t}$ and $\lim_{s\to 0}(H'(s)) = -\sqrt{\xi_\mathrm{c}k_\mathrm{i,c}}/k_\mathrm{i,c}$ and obtain

$$\kappa_\mathrm{aa} = 2\frac{\sqrt{\xi_\mathrm{t}k_\mathrm{i,t}}}{k_\mathrm{i,t}}\left(\frac{\sqrt{\xi_\mathrm{t}k_\mathrm{i,t}}}{k_\mathrm{i,t}} + \frac{\sqrt{\xi_\mathrm{c}k_\mathrm{i,c}}}{k_\mathrm{i,c}}\right)^{-1}. \tag{B.3}$$

In the same manner, we carry out all the other DC gains

$$\kappa_\mathrm{ab} = \left(\frac{\sqrt{\xi_\mathrm{t}k_\mathrm{i,t}}}{k_\mathrm{i,t}} - \frac{\sqrt{\xi_\mathrm{c}k_\mathrm{i,c}}}{k_\mathrm{i,c}}\right)\left(\frac{\sqrt{\xi_\mathrm{t}k_\mathrm{i,t}}}{k_\mathrm{i,t}} + \frac{\sqrt{\xi_\mathrm{c}k_\mathrm{i,c}}}{k_\mathrm{i,c}}\right)^{-1}, \tag{B.4}$$

$$\kappa_\mathrm{ba} = \left(-\frac{\sqrt{\xi_\mathrm{t}k_\mathrm{i,t}}}{k_\mathrm{i,t}} + \frac{\sqrt{\xi_\mathrm{c}k_\mathrm{i,c}}}{k_\mathrm{i,c}}\right)\left(\frac{\sqrt{\xi_\mathrm{t}k_\mathrm{i,t}}}{k_\mathrm{i,t}} + \frac{\sqrt{\xi_\mathrm{c}k_\mathrm{i,c}}}{k_\mathrm{i,c}}\right)^{-1}, \tag{B.5}$$

$$\kappa_\mathrm{bb} = 2\frac{\sqrt{\xi_\mathrm{c}k_\mathrm{i,c}}}{k_\mathrm{i,c}}\left(\frac{\sqrt{\xi_\mathrm{t}k_\mathrm{i,t}}}{k_\mathrm{i,t}} + \frac{\sqrt{\xi_\mathrm{c}k_\mathrm{i,c}}}{k_\mathrm{i,c}}\right)^{-1}. \tag{B.6}$$